traction had been established, barium chloride was removed by repeated washing with fresh Tyrode solution. Several washes were necessary to return tissue contraction back to the base line. After the tissue had stabilized, a given dose of the test compound was added and allowed 10 min for equilibration. Without washing out the test compound, an identical dose of barium chloride (300 μg/mL) was added, and contractions were recorded. The difference between smooth muscle contraction induced by barium chloride before and after the administration of the test compound was calculated in terms of percent inhibition.

Acknowledgment. We are grateful to Richard Dvorak for obtaining the mass spectra and to Dr. Michael T. Flavin and Marion Sitt for their help in the preparation of this manuscript.

Registry No. (±)-**1**, 105401-26-1; (±)-**1**·HCl, 50700-19-1; (−)-**1a**, 99545-92-3; (−)-**1a**·HCl, 50700-18-0; (+)-**1b**, 99553-27-2; (+)-**1b**·HCl, 50700-17-9; (±)-**2**, 105401-27-2; (±)-**2**·HCl, 105401-33-0; (−)-**2a**, 105497-78-7; (−)-**2a**·HCl, 105497-79-8; (+)-**2b**, 105498-87-1; (+)-**2b**·HCl, 105498-88-2; (±)-**3**, 105401-28-3; (±)-**3**·HCl, 105401-34-1; (±)-**4**, 105401-29-4; (±)-**4**·HCl, 105401-35-2; (±)-**5**, 105401-30-7; (±)-**5**·HCl, 105401-36-3; (±)-**6**, 105401-31-8; (±)-**6**·HCl, 105401-37-4; (±)-**7**, 105401-32-9; (±)-**7**·HCl, 105401-38-5; (±)-**8**, 31917-13-2; (+)-**8**, 28968-34-5; (−)-**8**, 59492-59-0; (±)-$C_6H_5C(CH_2OH)(CH_3)CO_2Et$, 70397-73-8; (±)-$C_6H_5C(CH_2Cl)(CH_3)COCl$, 105401-39-6; $Et_2N(CH_2)_2OH$, 110-73-6; $Et_2N(CH_2)_2Cl$, 100-35-6.

The Mechanism of Activation of 4-Hydroxycyclophosphamide

Richard F. Borch* and Jo Ann Millard

Department of Pharmacology and the Cancer Center, University of Rochester School of Medicine and Dentistry, Rochester, New York 14642. *Received June 9, 1986*

4-Hydroxycyclophosphamide (**2**/**3**) of unknown stereochemistry is the initial metabolite formed after administration of cyclophosphamide (**1**). Ultimate conversion to the cytotoxic metabolite phosphoramide mustard (**6**) is initiated by ring opening of 4-hydroxycyclophosphamide to produce aldophosphamide (**4**). The ring-opening reaction and subsequent equilibration of **2**–**4** are subject to general-acid catalysis, and the equilibrium composition is independent of buffer structure and pH. In contrast, formation of **6** from **4** proceeds by general-base-catalyzed β-elimination. *trans*-4-Hydroxycyclophosphamide undergoes ring opening ca. 4 times faster than the cis isomer, and cyclization of **4** favors the trans isomer by a factor of ca. 3 over the cis isomer. The rapid equilibration of **2**–**5** and the absence of elimination to give **6** at pH ~5 provides a convenient method to prepare a stable equilibrium mixture of activated cyclophosphamide metabolites suitable for in vitro use.

Cyclophosphamide (**1**) and its analogues are of considerable interest because of their therapeutic efficacy in the treatment of cancer and for the complexity of the activation mechanism that they undergo. The overall activation process has been reviewed;[1-3] more recently, we[4] and others[5] have described the mechanistic details of this process. Activation is initiated by hepatic cytochrome P-450 oxidation, and the resulting 4-hydroxy compounds **2** and/or **3** (see Scheme I) establish an equilibrium with aldophosphamide (**4**) and its hydrate **5**. General-base-catalyzed elimination of phosphoramide mustard from **4** is the rate-limiting activation step under physiologic conditions.[4,5,7] Enzymes are not required for catalysis after the initial hydroxylation. Intermediates **2**–**5** can be oxidized further to produce inactive metabolites. Although the aldehyde is clearly the pivotal intermediate in the activation process, it represents <5% of the metabolite mixture at equilibrium. Imine **9** has been identified as a transient intermediate in the enzymatic activation of **1**,[8] in the hydrolysis of 4-hydroperoxycyclophosphamide,[9] and in the activation of the 4-alkylthio-substituted analogue mafosfamide.[10] Compounds substituted with thiol groups at the 4-position show clinical promise as "preactivated" analogues[11] and may have significance as in vivo metabolites of **1**. We describe here our studies of the **2**–**5** equilibrium that demonstrate the importance of both acid- and base-catalyzed processes to cyclophosphamide activation; the chemistry of mafosfamide is presented in the accompanying paper.[10]

Table I. Equilibrium Constants for *cis*-**2** and *trans*-4-Hydroxycyclophosphamide (**3**) and Aldophosphamide + Hydrate (**4** + **5**)[a]

buffer (pH)	2/4 + 5	3/4 + 5	2/3
acetate (4.3–5.3)	2.28 ± 0.20	1.68 ± 0.07	1.36 ± 0.12
cacodylate (5.4–7.3)	2.55 ± 0.36	1.70 ± 0.19	1.50 ± 0.19
citrate (5.0–6.3)	2.61 ± 0.19	1.83 ± 0.13	1.43 ± 0.14
phosphate (5.3–7.0)	2.68 ± 0.24	1.82 ± 0.15	1.47 ± 0.14
mean	2.53 ± 0.17	1.76 ± 0.08	1.44 ± 0.06

[a] Mean ± SEM for at least six time points per experiment and at least four experiments at different pH values for each buffer.

Results and Discussion

cis-4-Hydroperoxycyclophosphamide (**13**) was synthesized in 40–50% reproducible yields according to the published procedure.[12] We have found the yields to be more consistent than with the method involving direct ozonolysis of cyclophosphamide.[9,13] *cis*-4-Hydroxycyclophosphamide

(1) Friedman, O. M.; Myles, A.; Colvin, M. *Adv. Cancer Chemother.* **1979**, *1*, 143–204.
(2) Stec, W. J. *Organophosphorus Chem.* **1982**, *13*, 145–174.
(3) Zon, G. *Prog. Med. Chem.* **1982**, *19*, 205.
(4) Borch, R. F.; Hoye, T. R.; Swanson, T. A. *J. Med. Chem.* **1984**, *27*, 490.
(5) Zon, G.; Ludeman, S. M.; Brandt, J. A.; Boyd, V. L.; Okkau, G.; Egan, W.; Shao, K-l. *J. Med. Chem.* **1984**, *27*, 466.
(6) Cis and trans refers to the relationship between the substituent and the phosphoryl oxygen, according to the convention established by: Kinas, R.; Pankiewicz, K.; Stec, W. J. *J. Org. Chem.* **1977**, *42*, 1650.
(7) Low, J. E.; Borch, R. F.; Sladek, N. E. *Cancer Res.* **1983**, *43*, 5815.
(8) Fenselau, C.; Lehman, J. P.; Myles, A.; Brandt, J.; Yost, G. S.; Friedman, O. M.; Colvin, O. M. *Drug Metab. Dispos.* **1982**, *10*, 636.
(9) Borch, R. F.; Getman, K. M. *J. Med. Chem.* **1984**, *27*, 485.
(10) Kwon, C.-H.; Borch, R. F.; Engel, J.; Niemeyer, U. *J. Med. Chem.* **1987**, *30*, 395.
(11) Kovach, J. S.; Svingen, P. A. *Invest. New Drugs* **1984**, *2*, 155 and other papers in this issue.
(12) Takamizawa, A.; Matsumoto, S.; Iwata, T.; Tochino, Y.; Katagiri, K.; Yamaguchi, K.; Sheratori, O. *J. Med. Chem.* **1975**, *18*, 376.

0022-2623/87/1830-0427$01.50/0

Scheme I

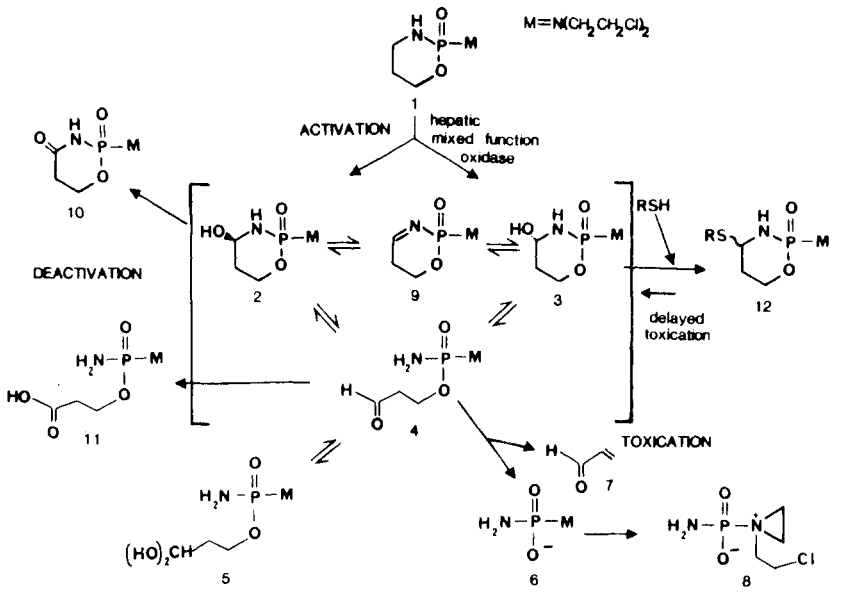

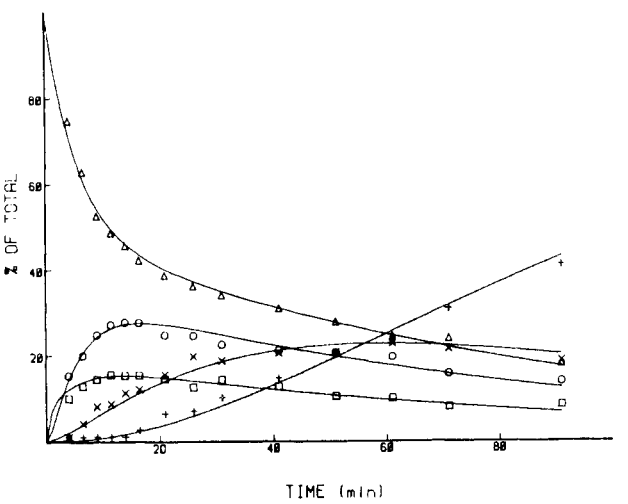

Figure 1. Activation of *cis*-4-hydroxycyclophospamide in phosphate buffer (0.1 M, pH 7.0, 37 °C). Data points were measured from ^{31}P NMR line intensities; the solid lines represent the best-fit values calculated by the Simplex algorithm. (△) **2**, (○) **3**, (□) **4** + **5**, (x) **6**, (+) PDA products.

(**2**) was prepared from **13** by reduction with dimethyl sulfide in a minimum volume of methanol followed by rapid addition of the appropriate aqueous buffer solution. ^{31}P NMR spectra were acquired as the reaction proceeded in the temperature-controlled NMR probe. The intermediates were quantified by peak intensity, and the rate constants were determined by nonlinear least squares methods using the Simplex Algorithm (see Experimental Section for details). The results of a typical experiment are shown in Figure 1, where the data points represent experimental values and the solid lines the calculated values based upon best-fit rate constants. In this example (0.1 M phosphate, pH 7.0, 37 °C) the equilibrium **2**–**5** is established after approximately 20 min, and the ratios of these intermediates remain essentially constant over the next 70 min. It should be noted that the resonances for aldehyde **4** and its hydrate **5** are not completely resolved in the ^{31}P NMR spectrum. However, the aldehyde/hydrate ratio was easily determined by ^{1}H NMR;[4] a value of

(13) Peter, G.; Wagner, T.; Hohorst, H.-J. *Cancer Treat. Rep.* **1976**, *60*, 429.

Scheme II

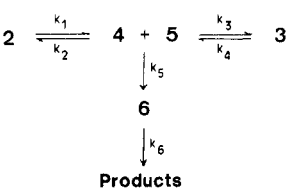

0.37 ± 0.04 was obtained under a variety of different buffer and pH conditions. Because **4** and **5** equilibrate at a rate that is very fast compared to the rates of the other reactions, aldophosphamide (**4**) is assumed to represent 27% [0.37/1.37] of the (aldehyde + hydrate) peak. The equilibrium constants were determined under a variety of conditions by measuring the ratios of **2**, **3**, and **4** + **5** at time points after the pseudoequilibrium had been established. These ratios were averaged, and a mean value for each set of buffer conditions was obtained. Ratios for individual time points were generally ± 10% of the mean for that experiment. Equilibrium constants for acetate, cacodylate, citrate, and phosphate buffers at different pH values are summarized in Table I. These data suggest that the pseudoequilibrium composition of intermediates **2**–**5** (48:33:5:14, respectively) is independent of buffer structure and pH.

The kinetic model for the activation process is shown in Scheme II and differential equations (1)–(5), where C,

$$dC/dt = -k_{1C} + k_{2AH} \quad (1)$$

$$dT/dt = k_{3AH} - k_{4T} \quad (2)$$

$$dAH/dt = k_{1C} + k_{4T} - AH(k_2 + k_3 + k_5) \quad (3)$$

$$dPDA/dt = k_{5AH} - k_{6PDA} \quad (4)$$

$$dPP/dt = k_{6PDA} \quad (5)$$

T, AH, PDA, and PP represent **2**, **3**, **4** + **5**, **6**, and phosphoramide mustard products (aziridinium ion **8** and solvolysis products), respectively. Examination of Scheme II indicates that equilibrium constants may also be obtained from the ratios of the best-fit rate constants. For all experiments the agreement between the values obtained by averaging data point ratios and those obtained by optimizing the rate constants was within 10%.

Having established the consistency of the pseudoequilibrium composition, we turned our attention to the ca-

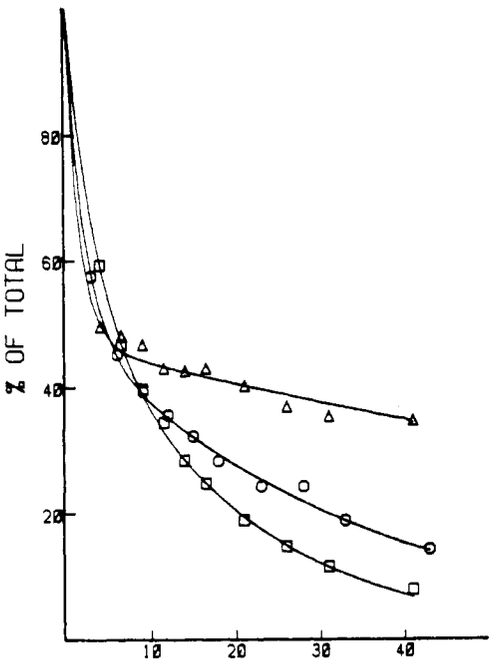

Figure 2. Reaction of *cis*-4-hydroxycyclophosphamide in phosphate buffer (0.4 M, 37 °C). Data points and solid lines were determined as in the legend to Figure 1. pH: (△) 5.3, (○) 6.2, (□) 7.0.

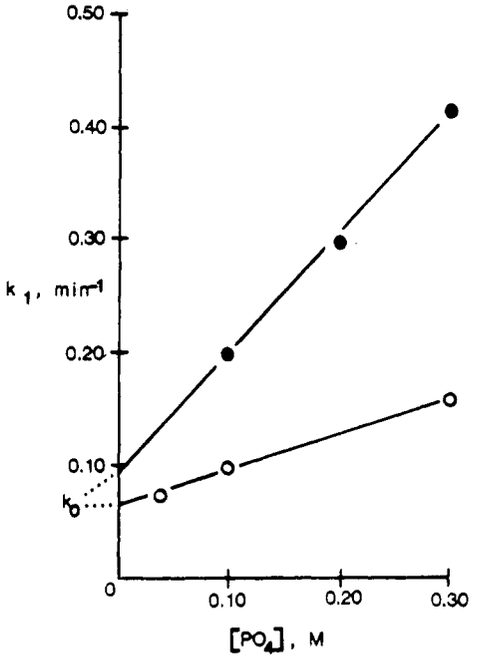

Figure 3. Effect of pH and buffer concentration on the rate constant for ring opening of *cis*-4-hydroxycyclophosphamide in phosphate buffer, 37 °C. (●) pH 5.3, (○) pH 7.0.

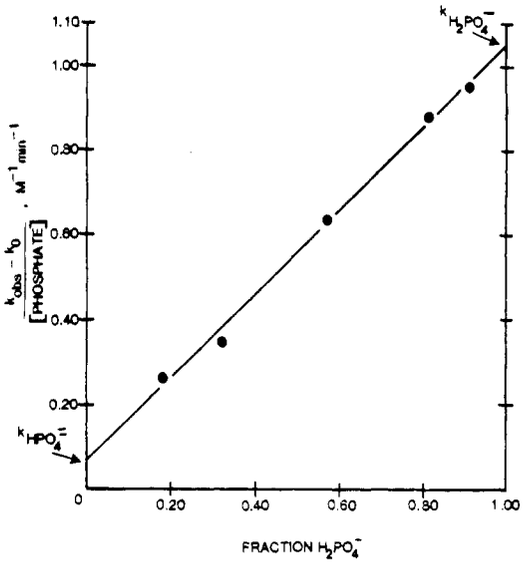

Figure 4. Effect of varying buffer composition on the catalytic rate constant for ring opening of *cis*-4-hydroxycyclophosphamide in phosphate buffer (0.4 M, 37 °C).

talysis of the ring-opening reaction, with emphasis on the effects of pH and buffer concentration on the rate constant k_1. Phosphate buffer provided reaction rates that were readily measurable by ^{31}P NMR, so this buffer was selected for these experiments. Reaction of *cis*-4-hydroxycyclophosphamide in phosphate buffer at pH 5.3–7.0 is shown in Figure 2. The disappearance of **2** is clearly biphasic. Initial ring opening of **2** is faster at pH 5.3 than at pH 7.0; after approximately 10 min, however, further disappearance of **2** is negligible at pH 5.3 but continues at pH 7.0. The early phase of this reaction is dominated by equilibration among **2**–**5** (vide infra); in contrast, the late reaction is dominated by elimination from **4** to give **6**. These data suggest that the initial ring-opening reaction is more rapid at lower pH and that the base-catalyzed elimination reaction is negligible at pH 5.3 as expected.[4,7] Equilibration is very rapid in acetate buffer (0.1 M, pH 5.0), and under these conditions elimination to **6** is not observed for at least 2 h. This provides a convenient method for the preparation of a metabolite mixture that is very useful for in vitro studies.

Rate constants for ring opening of **2** were determined at different pH and buffer concentrations; the results are shown in Figure 3. The ring-opening reaction is subject to acid catalysis, and the different non-zero intercepts for k_1 extrapolated to zero buffer concentration indicate that both H_2O and H_3O^+ are catalytically active in this reaction. The solvent rate constants k_0 obtained at different pH values can be used to determine the individual contributions from water and hydronium ion; the rate constants k_w and k_a thus obtained were 1.4×10^{-3} and 5.32×10^3 M^{-1} min^{-1}, respectively.

Rate constant k_1 (Scheme II) was determined at five different pH values, the solvent contribution to the reaction rate was subtracted, and the adjusted rate constant was corrected for buffer concentration to give the phosphate catalytic constant. This constant was then plotted against the fraction of $H_2PO_4^-$ present at each pH (Figure 4). The catalytic constants for $H_2PO_4^-$ and HPO_4^{2-} are 1.05 and 0.066 M^{-1} min^{-1}, respectively. Figure 5 shows a Brønsted plot for water, hydronium ion, and mono- and dihydrogen phosphate. The slope of the Brønsted plot $\alpha = 0.37$, indicating that the ring-opening reaction is general-acid catalyzed and that there is significant bond breaking in the transition state.

The rate constants k_2–k_4 obtained by nonlinear least squares analysis showed similar dependence on pH and buffer concentration. All rate constants increased linearly with increasing buffer concentration (phosphate, pH 7.4, 37 °C; Figure 6); the ordinate intercept values correspond to the solvent-catalyzed rate constants, and the slope provides the phosphate $k_{cat.}$ for each reaction. The values obtained for catalytic constants k_1–k_4 are 0.33, 0.72, 2.21, and 1.35 M^{-1} min^{-1}, respectively. Ring closure is much faster than ring opening for both cis and trans isomers as expected from the equilibrium constants. The rate of ring opening is ca. 4 times faster for *trans*- than for *cis*-4-

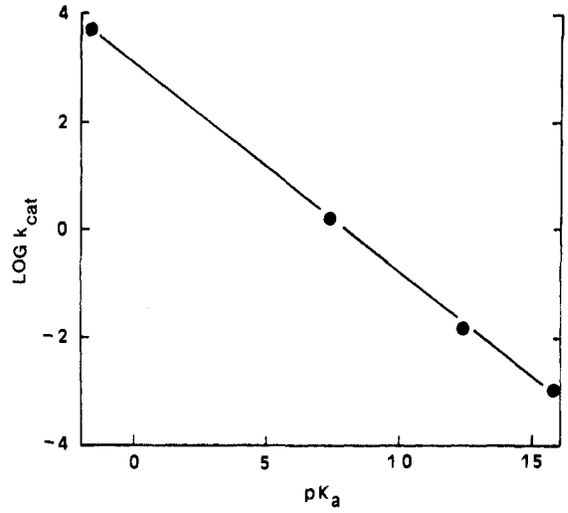

Figure 5. Brønsted plot for the acid-catalyzed ring opening of *cis*-4-hydroxycyclophosphamide at 37 °C. Data are for the following catalysts (left to right): H_3O^+, $H_2PO_4^-$, HPO_4^{2-}, H_2O.

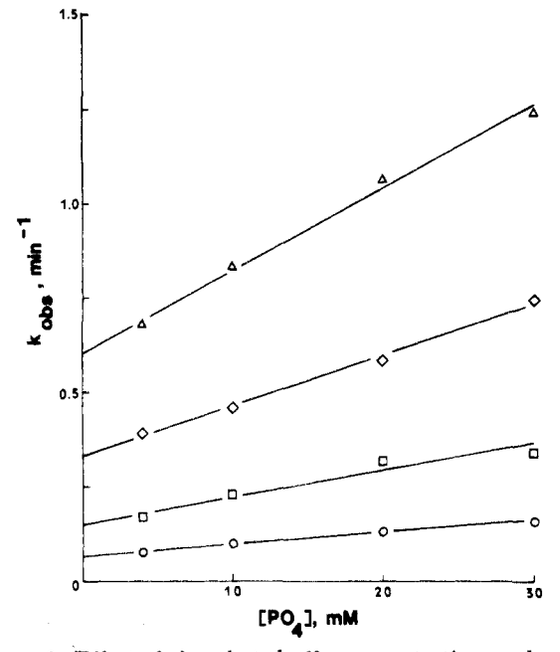

Figure 6. Effect of phosphate buffer concentration on the rate constants k_1–k_4 for interconversion of **2**, **3**, and **4** + **5** (pH 7.0, 37 °C; see Scheme II). (○) k_1, (□) k_2, (△) k_3, (◇) k_4.

hydroxycyclophosphamide, and aldophosphamide cyclizes to the trans isomer ca. 3 times faster than to the cis isomer. These results provide quantitative support for the relative cyclization rates suggested in our previous paper.[4] It is interesting to note that the less stable 4-hydroxy isomer is favored kinetically; although there are no apparent steric reasons for this preference, the protonated aldehyde may be stabilized (and therefore less reactive) by hydrogen bonding to the phosphoryl oxygen in the conformation leading to the cis product. In contrast, cyclization of the hemithioacetal kinetically favors *cis*-mafosfamide (cis/trans = 1.6).[10] In this case, stabilization by phosphoryl oxygen is not possible. Alternatively, formation of the thiironium ion from hemithioacetal may be rate limiting for this cyclization.

These findings lead to several important conclusions regarding cyclophosphamide activation. First, the stereochemistry of the hydroxylation reaction is probably not significant in vivo because under these conditions the *cis*- and *trans*-4-hydroxy isomers rapidly equilibrate. Second, the presence of a general-acid catalyst is not necessary for drug activation, since the water-catalyzed ring-opening reaction proceeds with a half-time of ca. 10 min. Finally, acidification of the urine should provide optimal protection against cyclophosphamide-induced bladder toxicity. Although acidification accelerates the initial equilibration step, formation of toxic metabolites is minimal at pH <6.

Experimental Section

Cyclophosphamide monohydrate, cacodylic acid and its sodium salt, and sodium phosphates were purchased from Sigma Chemical Co.; sodium acetate was obtained from Mallinckrodt. Other organic reagents and solvents were obtained from Aldrich Chemical Co. ^1H NMR spectra were recorded on an IBM WP-270-SY instrument using 5-mm sample tubes, a 4000-Hz spectral width, a 3-μs pulse width, a 2-s repetition time, and 64 scans. Improved sensitivity was obtained in some spectra by suppression of the residual HOD peak by using homonuclear gated decoupling. Chemical shifts are reported in parts per million from internal Me_4Si ($CDCl_3$) or 1-(trimethylsilyl)propanesulfonate (D_2O). ^{31}P NMR spectra were recorded on the same instrument equipped with an IBM-VSP multinuclear probe set for 109.368 MHz with 10-mm sample tubes, a 5000-Hz spectral width, a 10-μs pulse width, a 0.8-s pulse repetition time, and 64 scans. Broad-band gated proton decoupling was used. A constant flow of nitrogen (400 L/h) warmed to 37 °C by an IBM VT1000 variable-temperature unit was maintained throughout the decoupling experiments. Sample temperatures were measured by immersion of a precalibrated thermocouple attached to the VTU. Sample temperatures were monitored during the course of the experiment by measuring the chemical shift difference between triphenylphosphine and triphenylphosphine oxide in toluene-d_8 contained in a coaxial tube. Chemical shift and temperature were correlated with use of a previously determined standard curve. Chemical shifts are reported in parts per million from 5% triphenylphosphine oxide in toluene-d_8. Acidity measurements were made on a Radiometer pH meter using a glass–calomel combination electrode; pD values represent the meter reading of D_2O solutions and are related to pH according to pH = pD + 0.4. Buffer solutions were maintained at 37 ± 0.1 °C by a VWR 1145 constant-temperature circulator. Water was purified with a Barnstead Nanopure II System.

***cis*-4-Hydroperoxycyclophosphamide (13).** *O*-3-buten-1-yl *N*,*N*-bis(2-chloroethyl)phosphorodiamidate was prepared as previously described.[4] A solution of the butenyl ester (2.74 g, 10 mmol) in 30 mL of acetone/H_2O (2:1) was cooled to 0 °C, and ozone was bubbled through the solution for 15 min. The solution was removed from the cooling bath, 3 mL of 30% hydrogen peroxide was added, and the mixture was allowed to stand at room temperature while conversion to **13** was monitored by ^{31}P NMR. After the mixture was allowed to stand for 24 h, the acetone was removed in vacuo and the remaining aqueous solution extracted with $CHCl_3$ (4 × 25 mL). The combined organic layers were dried over $MgSO_4$, filtered, and evaporated in vacuo at 0 °C. The clear viscous oil was crystallized by the addition of a small amount of CH_2Cl_2 followed by Et_2O. The crystallization was completed at −20 °C. The crystals were collected by vacuum filtration, washed with Et_2O, and dried under vacuum: yield 1.22 g (42%), white crystals pure by ^1H and ^{31}P NMR and TLC, mp 97 °C (lit.[12] mp 107–108 °C).

NMR Studies. Except as noted, NMR studies were carried out as described previously.[4] All ^{31}P NMR studies were conducted at 37 ± 2 °C and μ = 1.0 ($NaNO_3$). Solutions of *cis*-4-hydroxycyclophosphamide (**2**) were prepared immediately prior to use by dissolving the appropriate quantity of **13** in approximately 50 μL of methanol and treating this solution with 13 μL of dimethyl sulfide at 37 °C. The appropriate buffer (2.5 mL, prewarmed to 37 °C) was then added to give a final concentration of 20 mM. The sample was then introduced into the preequilibrated spectrometer probe, and the spectra were acquired at varying intervals over 40–90 min. Time points for each spectra were taken at the midpoint of data acquisition. The FID spectra were stored on disk and subsequently processed by exponential multiplication with 2 Hz of line broadening, and relative concentrations of intermediates were determined from the peak heights of their

respective phosphorus resonances.

Determination of Rate Constants. Rate constants were determined by simultaneous fit of the experimental data points to the values calculated using the differential equations (1)–(5). A computer program was written by employing the Simplex algorithm[14] to optimize the rate constants by nonlinear least squares minimization. Calculated data points were determined every 6 s for the first 10 min, every 30 s for the next 15 min, and every minute for the remaining time points. Constants k_1–k_4 were optimized by using weighting factors of 1, 1, 1, 0.3, and 0.3 for intermediates **2**, **3**, **4** + **5**, **6**, and **8**, respectively (see Scheme I).

(14) Caceci, M. S.; Cacheris, W. P. *Byte* **1984**, *9* (No. 5), 340.

Acknowledgment. Financial support provided by Grants CA-11198 and CA-34619 from the National Cancer Institute, DHHS, is gratefully acknowledged.

5-Amino-4-(diazoacetyl)-1-β-D-ribofuranosylimidazole, a New Antileukemic Agent

H. Jeanette Thomas, Lisa N. Avery, R. Wallace Brockman, and John A. Montgomery*

Kettering-Meyer Laboratory, Southern Research Institute, Birmingham, Alabama 35255. *Received June 2, 1986*

5-Amino-4-(diazoacetyl)-1-β-D-ribofuranosylimidazole (**15**), 5-amino-4-(chloroacetyl)-1-β-D-ribofuranosylimidazole (**16**), and a number of related imidazole ribonucleosides have been synthesized. Compounds **15** and **16** are cytotoxic to both H.Ep.-2 and L1210 leukemia cells in culture. The (diazoacetyl)imidazole **15** is also active against the P388 leukemia in mice.

Azaserine and 6-diazo-5-oxonorleucine (DON) inhibit a wide variety of experimental neoplasms and have shown activity in humans, presumably curing choriocarcinomas.[1] These compounds are glutamine antagonists interfering with a number of enzymes involved in the de novo pathways to purine and pyrimidine nucleotides. The enzyme most sensitive to their action appears to be phosphoribosylformylglycinamidine synthetase (E.C. 6.3.5.3), which they irreversibly inactivate through the reaction of the diazomethyl group with a thiol of the enzyme active site.[2] It is this inhibition that is thought to be responsible for the antineoplastic activity of these compounds. Their structures are the basis of the design of imidazoles such as 5-amino-4-(diazoacetyl)-1-β-D-ribofuranosylimidazole (**15**) as potential anticancer agents that might act, for example, by interfering with the enzymic reaction catalyzed by *N*-(5-amino-1-β-D-ribofuranosylimidazole-4-carbonyl)-L-aspartic acid 5′-phosphate synthetase (E.C. 6.3.2.6). Since 5-amino-1-β-D-ribofuranosylimidazole-4-carboxamide is phosphorylated by adenosine kinase,[3] which is ubiquitous, it seemed reasonable to assume that this closely related structure would also be phosphorylated in cells, a potential prerequisite for significant inhibition of this enzyme. For this reason, we undertook the synthesis of **15**.

5-Amino-1-β-D-ribofuranosylimidazole-4-carboxamide (**1**) was transformed by the method of Robins et al.[4] to 5-amino-1-(2,3,5-tri-*O*-acetyl-β-D-ribofuranosyl)imidazole-4-carboxylic acid (**3**), which was converted to the acid chloride **4** by treatment with thionyl chloride (Scheme I). Since reaction of **4** with potassium *tert*-butoxide and nitromethane gave only the *tert*-butyl ester **9**, it was converted to 5-amino-4-(imidazol-1-ylacetyl)-1-β-D-ribofuranosylimidazole (**10**), which reacted readily with ammonia to give **1**, but neither **10** nor its derivatives blocked with either a trifluoroacetyl or phthaloyl group on the 5-amino group would react as desired with potassium *tert*-butoxide and nitromethane.[5] Reaction of **4** with diazomethane was also unsuccessful, giving the methyl ester **8** with only a trace of the desired (diazoacetyl)-imidazole **14**. Since interference by the amino group adjacent to the acid chloride of **4** seemed likely, it was blocked (in **3**) by formylation and by trifluoroacetylation, the latter procedure giving the mixed anhydride as well. Since neither of these intermediates, both still containing one proton of the amino group, could be converted to the desired (diazoacetyl)imidazole, phthaloylation of **3** was attempted. Because this attempt resulted in decarboxylation, the free acid (**3**) was converted by treatment with benzyl bromide and potassium carbonate in DMA to its benzyl ester (**7**), which could also be prepared by the reaction of **4** with benzyl alcohol. Reaction of **7** with [(ethoxycarbonyl)oxy]phthalimide gave the phthaloyl derivative **6**, which was debenzylated to the free acid **5**. Conversion of **5** to the acid chloride **11** followed by treatment with diazomethane gave the (diazoacetyl)imidazole **12**, which, on the basis of NMR and TLC data, is contaminated with a small amount of the chloromethyl ketone **13**. The phthaloyl and acetyl protective groups were removed from **12** by treatment with hydrazine, followed by ethanolic ammonia, to give the desired 5-amino-4-(diazoacetyl)-1-β-D-ribofuranosylimidazole (**15**). A slight excess of dry hydrogen chloride at room temperature converted **15** to the chloromethyl ketone **16**. Attempts to catalytically reduce the diazomethyl ketone **15** to the aminomethyl ketone **17** gave only the methyl ketone **18**.

Biologic Data

The diazomethyl ketone **15** inhibited the growth of both H.Ep.-2 and L1210 cells in culture with I_{50} values of 2 and 3 μM, respectively.[6] It also gave an 84% ILS of mice inoculated ip with 10^6 P388 leukemia cells when given qd 1–5 ip (100 mg/kg per dose).[6] It was less active given day 1 only (40% at 100 mg/kg) or q 3 h × 8 on days 1, 5, and 9 (61% ILS at 22.5 mg/kg per dose, 540 mg total dose). That a reactive group is essential to activity is attested to

(1) Bennett, L. L., Jr. *Handb. Exp. Pharmakol.* **1975**, *38*(2), 484.
(2) Buchanan, J. M.; Hartman, S. C. *Adv. Enzymol.* **1959**, *21*, 199 and references cited therein.
(3) Miller, R. L.; Adamczyk, D. L.; Miller, W. H.; Koszalka, G. W.; Rideout, J. L.; Beacham, L. M., III; Chao, E. Y.; Haggerty, J. J.; Krenitsky, T. A.; Elion, G. B. *J. Biol. Chem.* **1979**, *254*, 2346.
(4) Srivastava, P. C.; Mancuso, R. W.; Rousseau, R. J.; Robins, R. K. *J. Med. Chem.* **1974**, *17*, 1207.
(5) Chan, E.; Putt, S. R.; Showalter, H. D. H.; Baker, D. C. *J. Org. Chem.* **1982**, *47*, 3457.
(6) Montgomery, J. A.; Thomas, H. J.; Brockman, R. W.; Elliott, R. D. *J. Med. Chem.* **1984**, *27*, 680.

0022-2623/87/1830-0431$01.50/0